Current Alzheimer Research, 2017, *14*, 1109-1122

RESEARCH ARTICLE

iTRAQ-based Proteomic Analysis of $APP_{Sw,Ind}$ Mice Provides Insights into the Early Changes in Alzheimer's Disease

Nan Li[1,2], Pinghong Hu[1], Tiantian Xu[1], Huan Chen[1], Xiaoying Chen[1], Jianwen Hu[3], Xifei Yang[4], Lei Shi[4], Jian-hong Luo[1] and Junyu Xu[1,*]

[1]*Center of Neuroscience, Key Laboratory of Medical Neurobiology of Ministry of Health, Zhejiang Province Key Laboratory of Neurobiology, Zhejiang University School of Medicine, Hangzhou, Zhejiang 310058, P.R. China;* [2]*Women's Hospital, School of Medicine, Zhejiang University, Hangzhou 310006, P.R. China;* [3]*Shanghai Applied Protein Technology Co., Ltd., Shanghai, P.R. China;* [4]*Key Laboratory of Modern Toxicology of Shenzhen, Medical Key Laboratory of Guangdong Province, Medical Key Laboratory of Health Toxicology of Shenzhen, Shenzhen Center for Disease Control and Prevention, Shenzhen, P.R .China;* [5]*JNU-HKUST Joint Laboratory for Neuroscience and Innovative Drug Research, Jinan University, Guangzhou 510632, P.R. China*

Abstract: ***Background:*** Several proteins have been identified as potential diagnostic biomarkers in imaging, genetic, or proteomic studies in Alzheimer disease (AD) patients and mouse models. However, biomarkers for presymptom diagnosis of AD are still under investigation, as are the presymptom molecular changes in AD pathogenesis.

Objective: In this study, we aim to analyzed the early proteomic changes in $APP_{Sw,Ind}$ mice and to conduct further functional studies on interesting proteins.

Methods: We used the isobaric tags for relative and absolute quantitation (iTRAQ) approach combined with mass spectrometry to examine the early proteomic changes in hippocampi of $APP_{Sw,Ind}$ mice. Quantitative reverse transcription polymerase chain reaction (RT-PCR) and immuno-blotting were performed for further validation. Finally, the functions of interesting proteins β-spectrin and Rab3a in APP trafficking and processing were tested by shRNA knockdown, in N2A cells stably expressing β-amyloid precursor protein (APP).

Results: The iTRAQ and RT-PCR results revealed the detailed molecular changes in oxidative stress, myelination, astrocyte activation, mTOR signaling and Rab3-dependent APP trafficking in the early stage of AD progression. Knock down of β-spectrin and Rab3a finally led to increased APP fragment production, indicating key roles of β-spectrin and Rab3a in regulating APP processing.

Conclusion: Our study provides the first insights into the proteomic changes that occur in the hippocampus in the early stages of the AD mouse model. In addition to improving the understanding of molecular alterations and functional cascades involved in early AD pathogenesis, our findings raise the possibility of developing potential biomarkers and therapeutic targets for early AD.

ARTICLE HISTORY

Received: April 20, 2017
Revised: June 13, 2017
Accepted: June 29, 2017

DOI:
10.2174/1567205014666170719165745

Keywords: iTRAQ, hippocampus, pre-symptom, $APP_{Sw,Ind}$ mice, APP/PS1 mice, Alzheimer's disease.

1. INTRODUCTION

Alzheimer's disease (AD) is one of the leading causes of death in people older than 65 years [1]. Postmortem examinations of AD patients' brain and magnetic resonance imaging studies have revealed that volume loss and atrophy are present in various brain regions, and initiate from the entorhinal cortex and hippocampus [2-7]. In addition to brain-imaging and experience-based examinations, the detection of reduced β-amyloid peptide (Aβ) levels, increased Tau and phospho-Tau levels, or a combination of these changes in cerebrospinal fluid (CSF) allow AD diagnosis sensitivity and specificity to reach up to 85%-94% [8]. Genetic testing also provides powerful evidence for AD diagnosis: mutations in β-amyloid precursor protein (APP) and presenilin 1/2 genes are closely associated with familial AD [9-12], and apolipoprotein E gene polymorphism was reported to show strong correlation with AD [13]. Moreover, the results of multiplex immunoassays performed using CSF samples or brain tissue extracts from AD patients have shown that $A\beta_{42}$ and kallikrein 6 can serve as convincing AD biomarkers [14-16].

Proteomic methodologies have grown rapidly in recent years and offer a comprehensive shortcut in identifying molecular disease phenotypes, drug targets, and clinical biomarkers. Two-dimensional gel electrophoresis (2-DE) was

*Address correspondence to this author at the Center of Neuroscience, Zhejiang University, 866 Yuhangtang Road, Hangzhou, P.R. China;
Tel: 86-571-88208248; Fax: 86-571-88208248; E-mail: junyu@zju.edu.cn

1875-5828/17 $58.00+.00

used to analyze the molecular phenotype of the brain in AD, and significant changes were detected in proteins related to certain key pathways, such as those of stress response, lipid transport, neuronal growth, glycolysis, and diabetes mellitus development [17]. However, 2-DE has limitations in detecting low-abundance proteins, hydrophobic proteins, and proteins beyond 8-200 kDa in size. In quantitative proteomics, the isobaric tags for relative and absolute quantitation (iTRAQ) labeling method is used for relative and absolute quantitation [18]. This method can be combined with other technologies, such as 2D-nanoLC-nanoESI-MS/MS quantitative proteomics, to determine the amount of proteins from various sources in a single experiment [19, 20]. Manavalan *et al*. used the assorted method and identified 31 proteins whose expression was markedly altered in the hippocampus, parietal cortex, and cerebellum of AD patients [21]. Among the identified proteins, gelsolin, tenascin-R, and AHNAK could develop into biomarkers in late-onset AD [21]. iTRAQ was also used to test plasma proteins in patients with mild cognitive impairment and AD [22]. Thirty proteins related to inflammatory response, cholesterol transport, and blood coagulation were found to be dysregulated, and afamin and Ig μ-chain C region were identified as novel potential biomarkers [22]. In addition, iTRAQ was used to investigate proteomic changes in the hippocampus and cortex of 16-month-old 3×TgAD mice [23]. Coincidently, upregulated proteins associated with synaptic transmission, energy management, and cytoskeletal dynamics were identified [23].

However, the reported studies primarily focused on the late stage of the disease, and the results obtained cannot be readily applied as biomarkers for early-stage AD. The detailed molecular changes in cellular physiology in the early pathogenesis of AD remain unclear. In this study, we conducted iTRAQ analysis in the hippocampus in 10- to 12-week-old $hAPP_{Sw,Ind}$ J20 mice. J20 mice harbor 2 mutations in human APP (Swe, Ind) [24]; in these mice, senile plaques are produced at 5 months [25] and are accompanied by the development of cognitive impairment and a decline in learning and memory [26]. The iTRAQ results revealed that hundreds of proteins showed marked expression changes in J20 mice relative to the controls, among which 54 showed expression changes greater than 20%. We further verified these changes for a subset of the identified proteins at the mRNA level in the hippocampus of J20 mice and APP/PS1 mice, another widely used AD mouse model [27]. Finally, based on the aforementioned results, we tested the function of the altered proteins, β-spectrin and Rab3a, in APP trafficking and processing in N2A/APP695 cells, and found that β-spectrin and Rab3a play key roles in both APP membrane insertion and degradation.

2. MATERIAL AND METHODS

2.1. Animals

The **$APP_{Sw,Ind}$** J20 mice were the gifts from Dr. Binggui Sun (Zhejiang University). APP/PS1 (APP_{Swe}, PS1dE9) mice were also received as gifts from Dr. Fude Huang (Shanghai Advanced Research Institute, CAS). All mice were confirmed by PCR genotyping. For iTRAQ study, we used female J20 mice aged 10-12 weeks. For immunoblotting, we used female J20 and APP/PS1 (APP_{Swe}, PS1dE9) mice aged 10 weeks. For quantitative RT-PCR, we used female J20 mice aged 13-18 weeks, and APP/PS mice with mixed genders aged 11-18 weeks. All wild-type control mice were littermates of the corresponding AD mice. All animal use procedures were approved by the Committees at Zhejiang University and Leeds University for the Care and Use of Laboratory Animals, and were in accordance with the standards set forth in the 8th edition of the *Guide for the Care and Use of Laboratory Animals* published by the National Academy of Sciences, the National Academies Press, Washington DC, United States of America.

2.2. Perfusion and Tissue Dissection

J20 and wild-type female mice aged 10-12 weeks were anesthetized by intraperitoneal injection with sodium pentobarbital (1 mg/mL). The diaphragm was opened to expose the heart and perfusion was performed with ice-cold 1× PBS (phosphate buffered saline) from the left ventricle until the effluent ran clear. After perfusion, the brain was carefully dissected out from the skull and placed on ice. The hippocampi were then quickly dissected from the brain for use in iTRAQ analysis, immunoblotting, or RNA extraction.

2.3. Protein Digestion, iTRAQ Labeling, SCX Chromatography, and MS/MS Analysis

Proteins for each sample were diluted in STD buffer (4% sodium dodecyl sulfate [SDS], 100 mM dithiothreitol [DTT], 150 mM trisaminomethane hydrochloride [Tris-HCl], pH 8.0), incubated in boiling water for 5 min, diluted with UA buffer (8 M Urea, 150 mM Tris-HCl, pH 8.0), and transferred to 30-kDa ultrafiltration tubes. The samples were centrifuged at 14,000 *g* for 15 min twice with UA buffer and 0.05 M iodoacetamide in UA buffer, incubated for 20 min in the dark, and centrifuged three times at 14,000 *g* for 10 min with the filters equilibrated with DS buffer (50 mM triethylammonium bicarbonate, pH 8.5). Finally, trypsin (Promega) diluted in DS buffer was added to each filter and incubated overnight at 37°C. The resulting peptides were collected through centrifugation, and iTRAQ labeling was performed according to the manufacturer's instructions (Applied Biosystems). Proteins from 3 wild-type and 3 J20 mice were labeled with reagents 113, 114, and 115 and reagents 116, 117, and 118, respectively.

Before performing LC-MS/MS analysis, peptides were separated from excess labeling reagents by performing strong cation-exchange (SCX) chromatography: peptides were dried in a vacuum concentrator, dissolved in SCX buffer A (10 mM KH_2PO_4 in 25% acetonitrile, pH 3.0), and loaded onto a Polysulfoethyl column (5 μm, 200 Å, PolyLC Inc., MD, USA) at a flow rate of 1 mL/min. Peptides eluted with elution buffer (10 mM KH_2PO_4, 500 mM KCl in 25% acetonitrile, pH 3.0) were desalted on C18 Cartridges (Empore™ SPE Cartridges C18, Sigma), concentrated using a vacuum concentrator, and resuspended in 40 μL of 0.1% (v/v) trifluoroacetic acid. A total of 10 μL of the solution was injected for nanoLC-MS/MS analysis, using an AB SCIEX TripleTOF 5600 MS system (Toronto, Concord, Canada) equipped with a splitless Eksigent nanoUltra 2D Plus nanoLC system and a cHiPLC Nanoflex microchip system (Dublin, CA, USA). Collision energies were calculated

on-the-fly for all precursor ions by using empirical equations based on mass and charge, and the Enhance iTRAQ function was switched on to improve the efficiency of collision-induced dissociation.

2.4. Cell Culture and Transfection

N2A/APP695 cell medium was composed of equal amounts of OptiMEM (Gibco #31985-070) and DMEM (Gibco #11965-092) supplemented with 5% fetal bovine serum (Gibco #26140-079) and 1% penicillin-streptomycin (Gibco #15140-122). To select stable cells, G418 (Gibco #1181-031) was added to the growth medium at 100 μg/mL. Cells were cultured in a water-jacketed incubator at 37°C and a humidified atmosphere of air/5% CO_2. Cells cultured in 12-well dishes were transfected with 2-4 μg of DNA in 120 μL of transfection medium composed of 50% OptiMEM and 50% DMEM by using Lipofectamine 2000 (Invitrogen). For transfection, the growth medium from the 12-well dishes was removed and replenished with 0.5 mL of transfection medium. After transfection for 3 h, 0.75 mL of N2A/APP695 medium was added to the dishes. Cells were harvested 36-48 h after transfection.

2.5. Plasmid Construction

Short hairpin RNA (shRNA) constructs were generated by annealing synthetic primer pairs and subcloning into pSuper vector (a gift from Dr. Ip, Hong Kong University of Science and Technology). The annealing primers for β-spectrin shRNA were as follows:

5′-GATCTCCcccgaagatttgatcgcaaTTCAAGAGAttgcgatcaaatcttcgggTTTTTGGAAC-3′

5′-TCGAGTTCCAAAAAcccgaagatttgatcgcaaTCTCTTGAAttgcgatcaaatcttcgggGGA-3′

The annealing primers for β-spectrin shRNA were as follows:

5′-GATCTCCgcgccaaggacaacattaaTTCAAGAGAttaatgttgtccttggcgcTTTTTGGAAC-3′

5′-TCGAGTTCCAAAAAgcgccaaggacaacattaaTCTCTTGAAttaatgttgtccttggcgcGGA-3′

2.6. Real-time Fluorescence Quantitative PCR

Hippocampal RNA was extracted using the Qiagen RNeasy mini kit. N2A/APP695 cell RNA was harvested using Trizol (Takara). After measuring the RNA concentration, template RNA was reverse-transcribed into complementary DNA (cDNA) using the QuantiTect reverse-transcription kit. The QuantiFast SYBR Green PCR kit (Qiagen) was used to examine the relevant messenger RNA (mRNA) level. Real-time fluorescence quantitative PCR was performed in a CFX96 TouchTM Real-Time PCR Detection System (Bio-Rad). For each gene, one pair of primers was designed (Supplementary Table **1**) and verified through RT-PCR and DNA gel imaging. Each reaction was performed using 3 duplicate samples. The relative expression of genes was quantified by calculating the Cq value by using the -ΔΔCt method, and *GAPDH* was used as a reference gene.

2.7. Immunoblotting

Brain tissue samples from separated brain regions were homogenized in 10 mM Tris-HCl (pH 7.4) and centrifuged at 14,000 *g* for 20 min at 4°C. Protein concentration was determined using a BCA Protein Assay Kit (Thermo 23225) and adjusted to 1 mg/mL. Cells were harvested using Laemmli sample buffer and fully scraped out using a cell scraper, and the collected cell samples were boiled for 5 min at 100°C.

The proteins were separated using 10% or 12% SDS-PAGE and transferred to polyvinylidene fluoride membranes (Bio-Rad). The membranes were blocked in 0.5% skim-milk powder dissolved in Tris buffered saline tween (TBST). Antibodies used for immunoblotting were APP C-terminus (1:3000, Ct15, HuaAn), β-spectrin (1:1000, Abcam), sAPPα (1:50, IBL), sAPPβ (1:50, IBL) and GAPDH (1:1000, Beyotime), and fluorescent secondary antibodies (1:5000, 680M, 680R, Pierce). Protein bands were visualized using an Odyssey Infrared Imaging system (LI-COR).

2.8. Immunocytochemistry

To examine total APP expression, cells were fixed using 4% PFA (paraformaldehyde) in PBS containing 4% sucrose for 15 min, permeabilized with 0.2% Triton X-100 in PBS for 10 min, blocked in 10% NDS (normal donkey serum, diluted in PBS) for 1 h, incubated with anti-APP antibody 6E10 (1:500 in 3% NDS; Covance) overnight at 4°C, and then incubated with fluorescent Cyanine 3-M secondary antibodies (1:500; Invitrogen). To examine cell-surface APP, cells were fixed in 2% PFA in PBS containing 4% sucrose without Triton X-100 treatment. Images were captured using a laser-scanning confocal microscope (Olympus, FV-1000).

2.9. Data Analysis

All LC-MS/MS data were processed using ProteinPilot software. The MS/MS data were used to search the ExPASy database by using the "thorough search" option. Data were normalized using ProteinPilot. All reported data were based on FDR ≤ 1% confidence for protein identification. Gene oncology (GO) analysis was performed by the Gene Ontology Consortium (http://geneontology.org/) [28, 29]. Gene names were submitted for enrichment analysis, and the unmapped gene IDs were then modified and searched using their synonyms. The significance of the representation of the functional groups in the genes in comparison to the reference list was assessed using the binomial test [30] with a cut-off of $P < 0.05$. The data were exported and presented as pie charts by Microsoft Excel. The peptide-enrichment analysis and peptide alignment to the full-length protein sequence were performed using MAFFT software version 7 [31]. The data were exported and further analyzed to draw the consensus sequence mapping diagram using Jalview software version 2 [32]. Protein bands in immunoblots were analyzed using ImageJ (National Institutes of Health). Fluorescence signals were analyzed using MetaMorph software. Data were statistically analyzed by using GraphPad Prism v5.0 (Graph-

Pad Software, USA) and conducting unpaired or paired Student's *t* tests. At least 3 replicates were performed for each experiment.

3. RESULTS

3.1. Global Protein-expression Differences Between Control and $APP_{Sw,Ind}$ Mice

To examine the early molecular alterations in AD, we used the iTRAQ approach and performed large-scale quantitative analysis on the $APP_{Sw,Ind}$ J20 mouse, a widely accepted AD mouse model. Because the hippocampus is one of the first brain regions damaged during the early stages of AD [3, 7, 33], we dissected out the hippocampi from control and J20 mice when the mice were 10-12 weeks old, *i.e.,* before the appearance of Aβ plaques [24]. The control and J20 hippocampal proteins were digested by trypsin and labeled at their free amine sites by using isobaric mass-tag labels (control: 113, 114, 115, J20: 116, 117, 118) and analyzed using liquid chromatography tandem-mass spectrometry (LC-MS/MS). The iTRAQ results identified more than 3000 proteins from each sample, among which 363 proteins showing significant changes in J20-mouse hippocampal samples examined (Table **1**). In addition, we were able to detect proteins with more than 20% or even 50% of expression changes in 10- to 12-week-old J20 mice hippocampus (Table **1**), indicating obvious changes take place during early development of AD.

To obtain an overall understanding of the basic biological properties of the identified proteins in J20 mice, we performed gene ontology (GO) analysis of the 131 protein-encoding genes with statistically significant expression level changes for more than 10% of the controls. The unmapped genes were re-searched with their synonyms, and finally all genes except 1 were mapped (Table **2**).

The GO data revealed that most of the altered proteins were proteins with binding or catalytic capabilities (Fig. **1A**). Proteins with catalytic activities mainly showed upregulated expression, while structural proteins showed more on down-regulated expression (Fig. **1A**). When grouped with their biological process properties, the altered proteins were found mostly involved in cellular, metabolic, and developmental processes, or in regulating molecular localization (Fig. **1B**). Proteins involved in metabolic processes, or in regulating localization were tended to be increased (Fig. **1B**); by contrast, proteins involved in cellular and developmental processes were downregulated in a greater population than those that were upregulated (Fig. **1B**). Intriguingly, cellular components analysis showed that there were increased levels of macromolecular complexes and membrane proteins in J20 mice, while extracellular region protein, organelle proteins, or cell part proteins (basic structural and functional proteins of all organisms) were prominently decreased (Fig. **1C**). Collectively, the GO classification results provided an overview showing that during the early stages of AD pathology, abundant changes are exhibited by changes in structural protein, membrane protein composition, extracellular matrix, and enzyme catalytic activities in the hippocampus.

3.2. Comparison of Protein Levels Between Controls and $APP_{Sw,Ind}$ Mice

To analyze the specific proteins altered in J20 mice in detail, we further screened the proteins based on their fold-changes in expression level. We identified 165 proteins that showed at least a 20% increase or decrease in expression, of which 54 showed significant changes (Supplementary Table **2**). Moreover, 15 proteins exhibited more than a 50% change in their expression levels (Table **3**). As an internal control, mouse endogenous APP did not display any clear expression change in J20 mice, whereas the exogenous human APP exhibited almost 3-fold increase compared to endogenous APP, indicating the successful transgenic expression of the $hAPP_{Sw,Ind}$ gene, as well as the reliable quantification of protein mass using iTRAQ.

From the table, we noted a 49.7% reduction in the expression level of myelin basic protein (Mbp), indicating that the neurons could undergo demyelination during the early pathogenesis of AD, even before the appearance of Aβ plaques. A similar phenomenon was also observed in the hippocampus of 3×TgAD mice [34]. Notably, GFAP, a glial marker protein, was prominently increased in J20 mice (Table **3**), indicating the astrocyte activation and reactive gliosis accompanying AD pathogenesis. Moreover, we observed increased expression of ephrin B3, procollagen, and cadherin proteins, which suggests that in early AD progression, the cell adhesion could be affected. The mechanistic target of rapamycin (mTOR) signaling pathway might also be involved. Lastly, increased expression of Plch2, Plbd2, dephospho-CoA kinase domain-containing protein (Dcakd), and AH receptor-interacting protein (Aip) indicated changes in basal metabolism in the J20 hippocampus, and the upregu-

Table 1. Quantification of proteins that showed expression-level changes. Protein numbers were determined based on expression-level changes in J20 mice as compared to wild-type mice. Significant change: proteins in J20 mice showing statistically significant changes relative to wild-type control; Student's *t* test, $P < 0.05$.

Classify	Percentage of Expression Level Change				
	>0%	>5%	>10%	>20%	>50%
Total number	774	674	432	167	15
Significant change	363	249	131	54	5
Decreased expression	458	396	227	67	1
Increased expression	316	278	205	100	14

Table 2. Gene-ontology mapping quality. Gene were submitted for enrichment analysis in Gene Ontology Consortium, and the unmapped gene IDs were then modified and searched using their synonyms. The unsuccessfully mapped gene was *Rpsa-ps10* (entry deleted).

Gene Groups	Before Modification		After Modification		Remark
	Mapped	Unmapped	Mapped	Unmapped	
Decreased	66	0	66	0	
Increased	61	4	64	1	reference disclosed

Table 3. List of proteins with expression-level change for larger than 50%. Fifteen proteins that showed larger than 50% expression-level change in J20 mice are listed together with gene names, protein names, ExPASy accession numbers, and expression-level quantification parameters; 5 of the proteins that showed significant changes are indicated by asterisks. Peptides (95%): number of detected peptides at >95% confidence; % Cov: percentage of coverage of peptides on identified proteins; % change: percentage change of protein-expression level in J20 mice as compared to that in wild-type mice. *P < 0.05, **P < 0.01: significant changes in protein-expression levels.

Gene Name	Protein Name	Accession #	Peptides (95%)	% Cov	% Change	*P* Value
GFAP	Glial fibrillary acidic protein	P03995	51	76.5	99.4	0.059
Mbp	Myelin basic protein	F6RT34	73	72.2	-49.7	0.068
Col1a2	Procollagen, type I, alpha 2	Q3TX57	17	29.8	59.5	0.154
Calb2	Calretinin	Q08331	11	56.8	133.6	0.221
Plch2	1-phosphatidylinositol 4,5-bisphosphate phosphodiesterase eta-2	F7C3A0	5	13.5	57.3	0.003
Cdh13	Cadherin 13	Q8VDK4	4	13.9	67.7	0.020
Aip	AH receptor-interacting protein	O08915	2	23.3	114.6	0.069
Dcakd	Dephospho-CoA kinase domain-containing protein	Q8BHC4	2	16.9	78.6	0.035
Atp2a1	Sarcoplasmic/endoplasmic reticulum calcium ATPase 1	Q8R429	12	23.7	216.6	0.206
Plbd2	Putative phospholipase B-like 2	Q3TCN2	1	6.9	88.0	0.065
Efnb3	Ephrin B3	Q543Q7	1	15.6	114.4	0.063
Fam81a	Protein FAM81A	Q3UXZ6	2	20.3	129.7	0.045
Abca9	ATP-binding cassette sub-family A member 9	Q8K449	0	7.5	54.3	0.089
Wdr77	Methylosome protein 50	Q99J09	1	5	78.0	0.154
APP	Amyloid beta A4 protein (human)	P05067-8	20	37.2	275.9	0.008
APP	Amyloid-beta protein-like protein long isoform (mouse)	Q53ZT3	19	34.2	-6.0	0.313

lation of methylosome protein 50 suggested potential epigenetic alterations in early AD.

We also examined the proteins that showed significant changes in expression of more than 20% of control mice level (Supplementary Table **2**). Myelin-associated glycoprotein (Mag), which is another myelination-associated protein, showed reduced expression, whereas raptor, a regulatory component in the mTOR pathway, showed a 19.7% increase in protein level. Additional changes in the signaling pathways in AD were suggested by a downregulation in the J20 hippocampus of certain transporters, protein tyrosine kinases, and the sodium channel subunit β-2 (Scn2b).

3.3. Validation of mRNA Expression Levels in AD Mouse Models

Next, we validates gene-expression changes at the mRNA level by quantitative RT-PCR in hippocampal samples obtained from J20 and another AD mouse model, the APP/PS1 (APP_{Swe}, PS1dE9) mice [27], at the age of 10-12 weeks. We examined 34 genes based on their expression

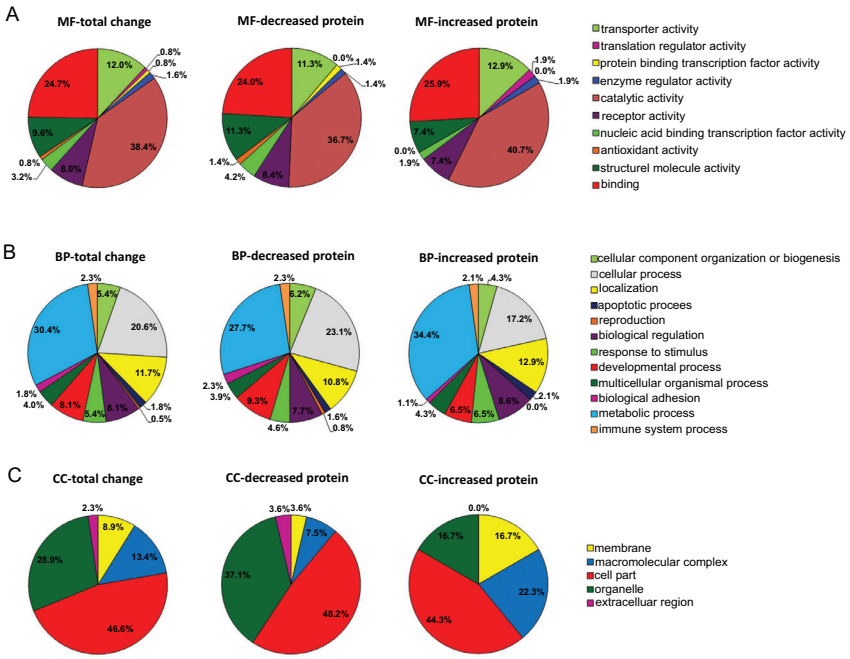

Fig. (1). Gene-ontology analysis of proteins showing altered expression in J20 mice. GO analysis was performed to classify the proteins that showed at least 10% of significant altered expression levels in the iTRAQ study. Populations of proteins that showed altered expression, increased expression, or decreased expression are indicated based on their GO for **(A)** molecular function, **(B)** biological process, and **(C)** cellular components.

changes and acknowledged associations with AD. The results of quantitative RT-PCR showed that these genes exhibited distinct patterns of expression. Accordingly, we classified the genes into 4 groups: (1) genes that showed a consistent change at both the protein and mRNA levels in both J20 and APP/PS1 mice (Fig. **2A**); (2) genes that showed a consistent change at both the protein and mRNA levels in J20 mice, but showed either no significant change or a reversed mRNA-level change in APP/PS1 mice (Fig. **2B**); (3) genes that showed a reversed change between protein and mRNA levels in J20 mice, but showed the same change in protein levels in J20 mice and mRNA levels in APP/PS1 mice (Fig. **2C**); and (4) genes that showed reversed changes between protein and mRNA levels in both mouse models (Fig. **2D**).

Genes in group 1 mostly included those associated with oxidative stress and neuro-protection. The expression of glial high-affinity glutamate transporter GLT-1 (gene name *Slc1a2*) was diminished in both mouse models and at both protein and mRNA levels (Fig. **2A**), which indicated defects in glial glutamate uptake. Similar reductions were also exhibited by peroxiredoxin 6 (Prdx6), an antioxidant enzyme expressed mainly in astrocytes [35], and sirtuin 2 (SIRT2), a recognized microtubule organizer and histone regulator that is associated with Huntington disease and Parkinson disease [36] (Fig. **2A**). Moreover, glutathione S-transferase μ-1 (Gstm1), an AD risk factor [37-39], showed a significant and consistent reduction in both mouse models (Fig. **2A**). Notably, 3 proteins closely related to AD and Lewy body spectrum disorders [40-45], limbic system-associated membrane protein (lsamp) and the neurotrophic and neuroprotective factors synuclein and S100b, were reduced in both the J20 and the APP/PS1 hippocampus (Fig. **2A**). We also found proteins with changes that differed from previous studies. S100b was found to be elevated in the temporal lobe of AD patients [46], but had a decreased expression in 2-month-old AD mice hippocampi (Fig. **2A**). Ubiquitin carboxyl-terminal esterase L1 (Uchl1) was reported to be reduced in the brain samples of sporadic AD patients [47], but we detected elevated Uchl1 expression at both the protein and mRNA levels in both AD mouse models (Fig. **2A**).

Among Group 2 genes, we found the gene encoding EF-hand domain-containing protein D2(EFhd2), a calcium-binding protein that was reported to form filamentous structures and co-aggregate with Tau proteins in AD brains [48]; EFhd2 exhibited increased expression in J20 mice, but the variation of the PCR product in APP/PS1 mice was too large to allow detection of any statistically significant change (Fig. **2B**). This result showed that a cytoskeleton dependent trafficking could be altered during early AD pathology of J20 mice.

Group 3 comprised genes encoding small G proteins, spectrins, and the SNARE protein N-ethylmaleimide-sensitive factor (Nsf), all of which showed reduced protein expression but increased mRNA levels in J20 mice, and reduced mRNA levels in APP/PS1 mice (Fig. **2C**). The inconsistency between the protein and mRNA expression levels might be due to differences in compensatory strategies of cells for core protein loss, or the intrinsic differences in gene transcription between the two mouse models.

We noted an interesting trend among Group 4 genes: the small G protein Rab3 and 2 proteins that associate with it, rabconnectin-3 (Dmxl2) and rabphilin 3A (Rph3a), showed reduced protein expression and increased mRNA expression.

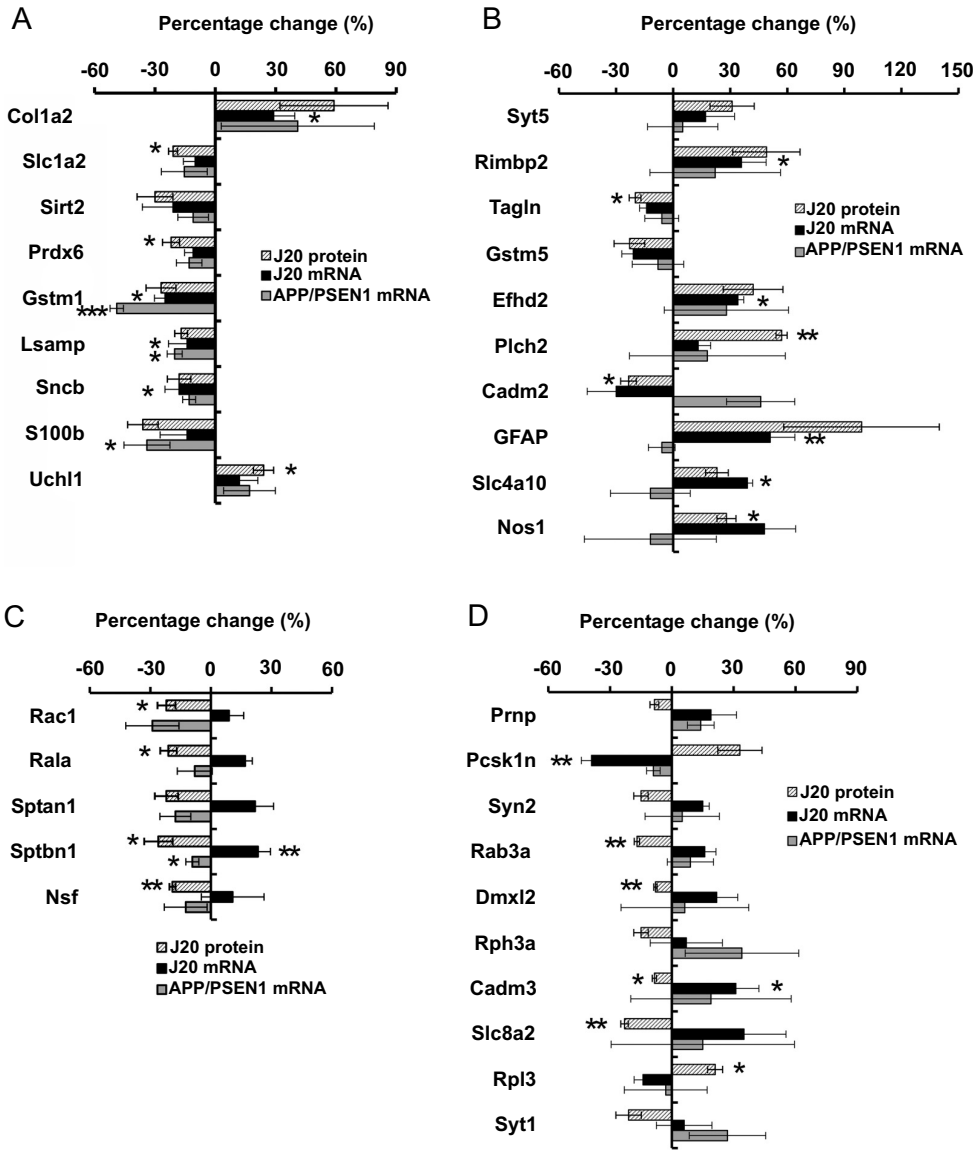

Fig. (2). Examination of mRNA expression of selected genes in J20 and APP/PSEN1 mice. Bar chart showing the mRNA expression of certain genes in the 2 mouse models, together with the protein-expression changes detected from the iTRAQ analysis. **(A)** Genes that showed a consistent change at the both the protein and mRNA levels in both J20 and APP/PSEN1 mice. **(B)** Genes that showed a consistent change at both protein and mRNA levels in J20 mice, but showed no correlated change in APP/PSEN1 mice. **(C)** Genes that showed a reversed change between protein and mRNA levels in J20 mice, but showed a consistent change in mRNA levels in APP/PSEN1 mice. **(D)** Genes that showed a reversed change between protein and mRNA levels in both mouse models. Error bars denote the SEM; Student's test, *P < 0.05, **P < 0.01, ***P < 0.001, compared to wild-type control; n = 3-7 replicates.

Because Rab3a and its associated complex have been reported to regulate the anterograde transport of APP [49], we consider these results to suggest a role of Rab3 functional complex in early AD pathology or to exerts a compensatory role under APP overexpression.

3.4. Validation of Protein Expression Levels in AD Mouse Models

To further confirm the validation of iTRAQ results, we examined the protein expression levels in J20 mice and other AD mouse models using the western blot approach. Elevated GFAP expression accompanied by astrogliosis is one of the hallmark proteins found to be elevated in CSF of AD and dementia patients [50-53]. Ubiquitin is one of the proteins we found to have different expression changes as previously reported [49]. We checked the GFAP and ubiquitin protein levels in hippocampus and cortex of J20 and APP/PS1 mice aged 10-12 weeks (Fig. **3**). Consistent with the qRT-PCR result, the immunoblotting result showed a prominent increase of GFAP expression in both hippocampus and cortex regions of J20 mice (Fig. **3A, B**), while its expression in APP/PS1 mice had no distinguishable change from WT mice (Fig. **3C, D**). For ubiquitin, we detected a consistent increase

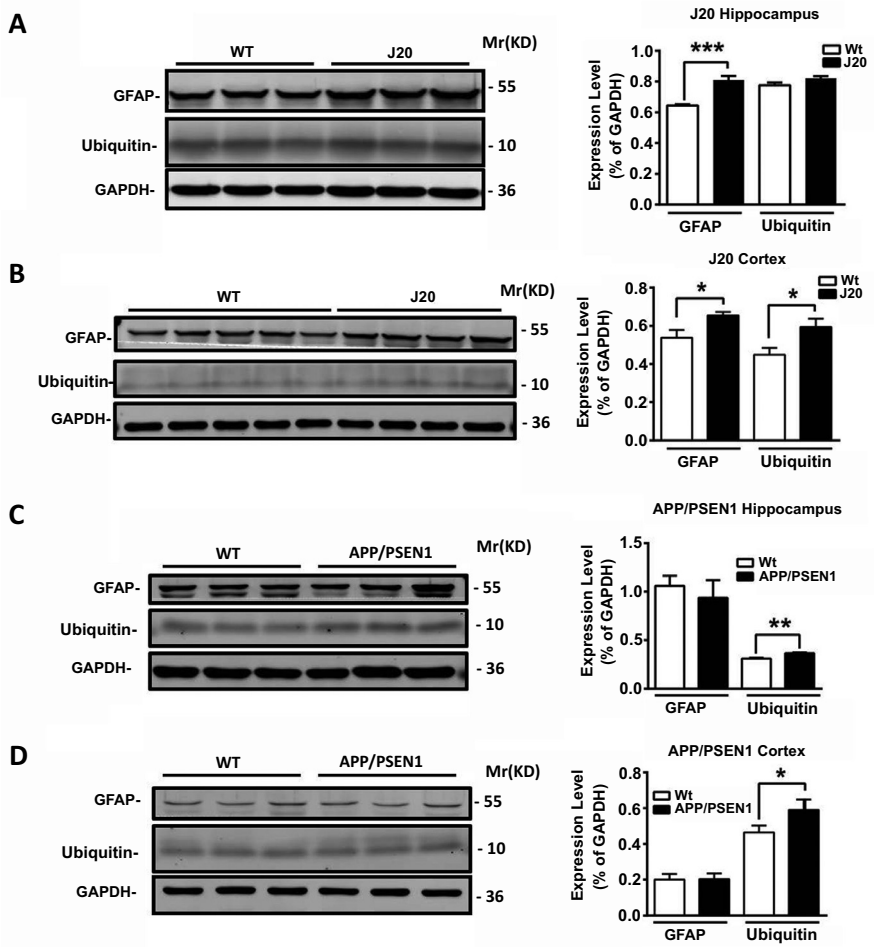

Fig. (3). Expression of GFAP and Ubiquitin in hippocampus and cortex regions of AD mice. **(A)** In hippocampus of J20 mice, GFAP has a remarkable increase, while Ubiquitin shows a slight but insignificant upregulation compared to wild-type. **(B)** In cortex of J20 mice, both GFAP and ubiquitin show significant upregulated expression. **(C)** In hippocampus **(C)** and in cortex **(D)** of APP/PSEN1 mice, GFAP keeps unaltered and Ubiquitin shows evidently increasement than wild-type mice. Error bars denote the SEM; Student's t test, *P < 0.05, ***P < 0.001, compared to wild-type control; n = 3-5 mice.

in both hippocampus and cortex of J20 and APP/PS1 mice compared to WT mice (Fig. **3**). Even though the increment of ubiquitin expression in J20 hippocampus did not show statistical significance, we observed a trend of increased expression (Fig. **3A**).

Spectrins were identified as one of the proteins deposited in Aβ plaques [54, 55]. α-spectrin was shown to be cleaved by calpain and caspase-3 and its 120-kDa breakdown product was increased in the aged brains from both AD patients and 3×TgAD mice [56-59], and is therefore considered as a potential AD biomarker [60]. Recently, β-spectrin was also found to be cleaved by calpain and caspase under neurotoxic and traumatic brain-injury conditions [61]. Our iTRAQ and qRT-PCR results showed that β-spectrin protein expression was diminished but the mRNA level was increased (Supplementary Table **2** and Fig. **2C**). The expression of this spectrin could have been diminished as the result of a reduction in the level of the full-length protein or the protein fragment. To clarify this, we determined the enrichment of β-spectrin peptides from the iTRAQ results. Every identified peptide was aligned with the β-spectrin full-length sequence, and with the peptides that showed more than a 20% or 50% change in quantity. The alignment results revealed that the identified peptides covered almost the entire β-spectrin sequence (Fig. **4A**, peptide hits). The peptides with expression-level changes were distributed evenly in protein, suggesting an overall reduction of the full-length protein (Fig. **4A**). Moreover, the increased peptide population did not show a clustering pattern resembling calpain- or caspase-cleaved fragments (Fig. **4A**). Therefore, the reduction of β-spectrin in our result could represent a general protein-degradation event instead of partial cleavage in the early stages of AD in the J20 mouse hippocampus.

We also examined the expression level of β-spectrin in distinct brain regions of 10-week-old J20 and APP/PS1 mice; the results showed that full-length β-spectrin was reduced slightly in the hippocampus of J20 mice and remarkably in the hippocampus and cortex region of APP/PS1 mice (Fig. **4B, C**). These results suggest that the reduction of β-spectrin is a common defect in J20 and APP/PS1 AD mouse models.

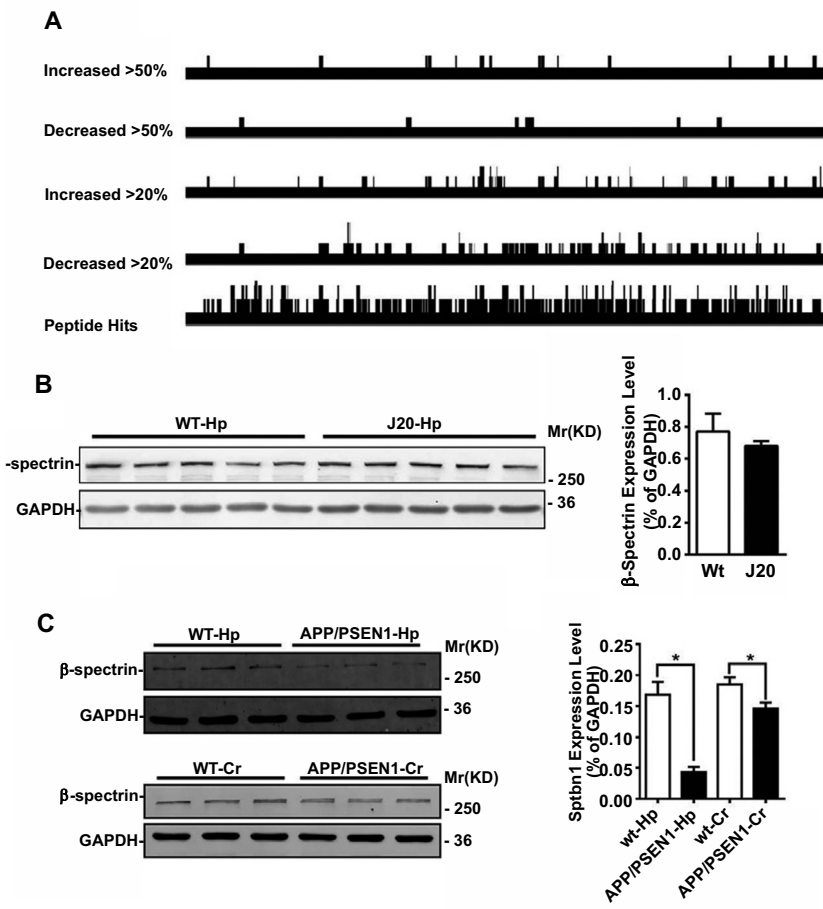

Fig. (4). Reduced expression of full-length β-spectrin in AD mice. **(A)** β-spectrin peptide-enrichment analysis from iTRAQ results. The full-length β-spectrin sequence is shown as long black lines. Peptides identified from iTRAQ that hit the β-spectrin sequence are shown as black bars on the corresponding region of alignment. The heights of the black bars represent the relative numbers of the identified peptide sequence. Peptides that showed quantity changes (>20% and >50%) between J20 and wild-type mice were also extracted for enrichment analysis. **(B)** Examination and quantification of β-spectrin expression levels in the hippocampus (Hp) of J20 mice. Error bars denote the SEM; n = 5 replicates. **(C)** Examination and quantification of β-spectrin expression levels in the hippocampus (Hp) and cortex (Cr) of APP/PSEN1 mice. Error bars denote the SEM; Student's t test, *p<0.05, compared to wild-type control; n=3 replicates.

3.5. β-spectrin and Rab3a Regulate APP Processing and Trafficking

Because β-spectrin plays an important role in vesicle transport [62, 63], we wondered if it is also involved in APP trafficking and AD pathology. We therefore used shRNAs to knockdown endogenous β-spectrin in neuroblastoma N2A cells stably expressing human APP695 protein (N2A/APP695 cells) [64]. Cells were cotransfected with shRNA plasmid together with a GFP-expressing plasmid, and the APP level was detected using both immunoblotting and immunostaining approaches. Successful knockdown of β-spectrin was demonstrated by the results of immunoblotting and qRT-PCR assays (Fig. **5A**). We found that β-spectrin depletion led to elevated proteolytic processing of APP, indicated by the increased APP C-terminal fragments (Fig. **5B**). We also detected a significant increase in soluble APP fragment sAPPα production and a trend of increase in sAPPβ production in the culturing medium of N2A/APP695 cells after β-spectrin knockdown (Fig. **5C**). The surface APP level was also elevated in N2A/APP695 cells after β-spectrin knockdown (Fig. **5D**). These results indicate that β-spectrin regulates APP trafficking and processing. The β-spectrin level should be maintained at an appropriate level to prevent both excessive cell-surface expression and excessive cleavage of APP. The reduced protein expression and elevated mRNA level of β-spectrin measured in J20 mice raised the possibility that through certain feedback pathways, AD cells might increase the β-spectrin transcript level to compensate for the protein loss.

In addition, we examined the function of Rab3a on APP expression and processing using the same approach, because it had been reported to regulate the anterograde transport of APP in axons [49]. A similar result was found on APP expression after Rab3a knockdown by RNAi. The total and soluble APP fragments were upregulated by Rab3a knockdown (Supplementary Fig. **1A**), as was the membrane APP level (Supplementary Fig. **1B**). The result showed that Rab3a also plays important role in APP degradation processing and protein expression.

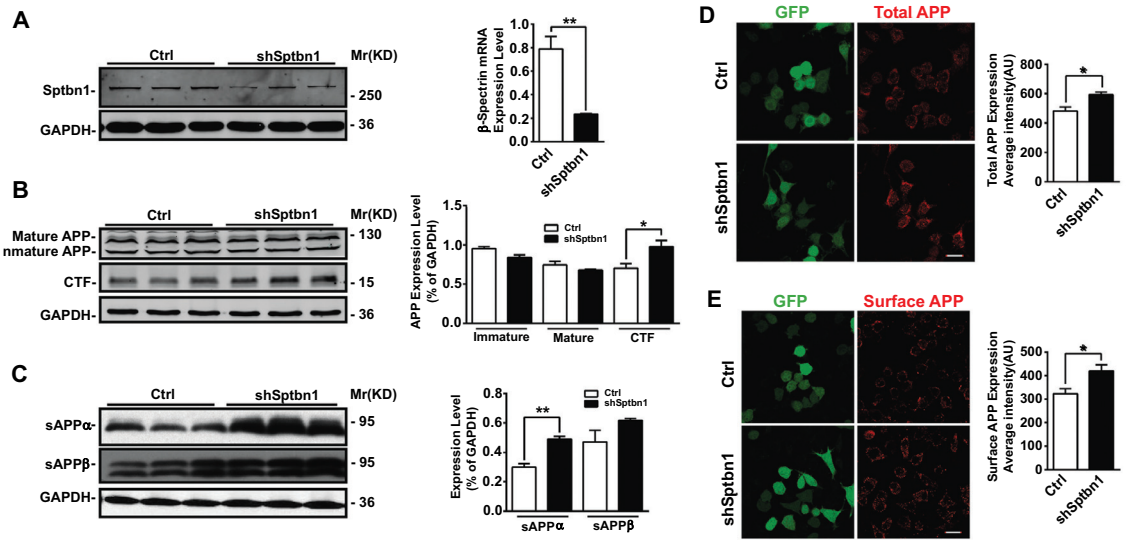

Fig. (5). Effect of β-spectrin knockdown on APP surface expression and cleavage. **(A)** Validation of β-spectrin knockdown by shRNAs in N2A/APP695 cells. Left panel: immunoblotting results showing shRNA-induced reduction of β-spectrin protein expression; right panel: quantitative RT-PCR results showing effective knockdown of β-spectrin mRNA. **(B)** Immunoblotting analysis and quantification of full-length APPs and APP C-terminal fragments expression in N2A/APP695 cells after β-spectrin knockdown. **(C)** Immunoblotting and quantification of sAPPα and sAPPβ in N2A/APP695 cells after β-spectrin knockdown. Immunocytochemistry results showing an increase in surface **(D)** APP levels after β-spectrin knockdown. Scale bar = 20 μm. Error bars denote the SEM; Student's t test, *P < 0.05, **P < 0.01; n = 3 replicates.

4. DISCUSSION

AD early diagnosis and intervention are critical but as yet unsatisfied requirements in AD treatment. Previous iTRAQ studies have identified alterations in inflammatory response, lipid transport, and neuronal growth in late AD pathogenesis [21-23]. Aβ42, total Tau, kallikrein 6, gelsolin, tenascin-R, AHNAK, afamin, and the Ig μ-chain C region have been identified as potential markers for AD diagnosis [14, 16, 17, 21-23]. However, all of these proteins were identified in the symptomatic stage of AD. In this study, we performed iTRAQ analysis on hippocampal proteins from 10- to 12-week-old $APP_{Sw,Ind}$ mice, which allowed us to observe the early molecular changes in this AD mouse model before morphological or behavioral symptoms. In addition to stimuli response- and neuronal growth-involved changes, we have also identified several biological functions altered in the early stages of AD progression, such as GFAP, Mag and Mog proteins for myelination and astrocyte activation. In addition to the aforementioned abnormalities, we detected the upregulation of proteins in the mTOR signaling pathways (Fig. **6**), and the downregulation of proteins of the Rab3 complex, which is involved in APP trafficking and exocytosis [49, 65, 66]. Insufficiency in the Rab3 level may lead to accumulation of intracellular APP and thereby increase the APP cleavage.

Another protein besides Rab3-complex proteins that was downregulated was full-length β-spectrin, accompanied by an upregulation of its mRNA level. It was not surprising that the increased β-spectrin fragment could not be detected in our study. As previously reported, the β-spectrin fragment accumulation was not found in 6-month-old mice, but was found in the 12 month-old ± 3xTg-AD mice and in elderly AD patients [56, 59]. The increased mRNA level of β-spectrin could also represent a cell-defense mechanism in early AD pathology. Spectrin serves as a scaffold protein for membrane proteins [67, 68]. One of the brain-specific beta-spectrins was also found to interact with Munc13 and be involved in neurotransmitter release and protein membrane delivery [62, 63]. Therefore, spectrin could also be involved in the membrane transport and stabilization of APP. To test this hypothesis, we knocked down the expression of endogenous β-spectrin by using shRNAs, and found that APP cleavage was increased. We think that once spectrin is knocked down, the APP will be maintained in trafficking vesicles or endosomes, which would facilitate its proteolytic cleavage. The β-spectrin level was probably diminished as a result of accelerated β-spectrin degradation, which led to increased APP proteolysis. Neurons could enhance the β-spectrin mRNA production through a feedback loop as a mechanism to decelerate the amyloid production and thereby attenuate the AD pathology.

As summarized in (Fig. **6**), our results provide insights into the possible changes in early AD hippocampus: Demyelination and astrocyte activation can occur before Aβ plaque formation. Glutamate releasing and axonal growth can be disturbed. Cell adhesion molecules were reduced to affect the spine formation. The Akt-mTOR signal pathway was affected, which facilitate amyloid deposition and reduce cell survival capability. The cells in the AD hippocampus could boost their metabolic and transcriptional activities, and increase their sensitivity to oxidative stress. Concurrently, the levels of synaptic and organelle proteins could diminish as apoptosis progresses.

It is worth mentioning that for Rac1, Rala, spectrins, and Nsf, we detected inconsistent changes between the mRNA and protein expression levels in J20 mice but not APP/PS1

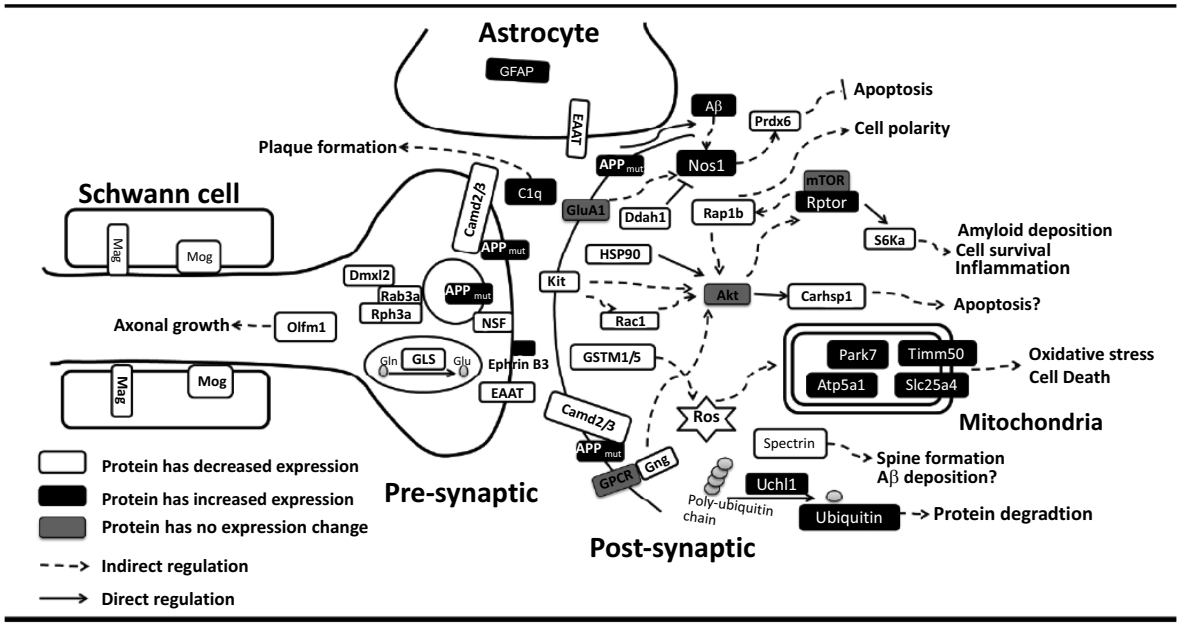

Fig. (6). Schematic diagram representing early changes in hippocampus of AD mice.

mice. These distinct mRNA changes in the two mouse models probably reflect dissimilar compensatory capabilities in different mouse models, or due to the overexpression effect of mutant PS1. The previously mentioned proteins play an important role in regulating vesicle trafficking, and a lack of these important functions may lead to a feedback effect of elevated gene transcription. Another possible explanation goes to their intrinsic gene expression differences in the two mouse models. In J20 mice, Aβ deposition starts between 4 and 5 months of age [24], and becomes extensively visible in cortex and hippocampus by 12 months [69]. The astrocyte activation and increased neurogenesis in hippocampus was detected as early as 3 months, and the elevated neurogenesis reverted when the mice became older [70, 71]. In APP/PS1 mice, Aβ deposition starts at 6 months of age [72]. The astrocyte activation could be detected by 8 months [73], which explains why the GFAP showed an increase in both protein and mRNA level in J20 mice but not in APP/PS1 mice in our results (Fig. 2 and Fig. 3). It is worth mentioning that the APP+PS1 mice had more severe spine loss than the J20 mice at the same age [74]. In addition, the behavioral study from the two mouse models showed distinct progression in memory deficits and cognition deficits by Webster *et al.* [75]. Therefore, the APP/PS1 mice have slower pathogenic progression than the J20 mice possibly due to the reason that some gene showed expression changes in J20 mice had no change in APP/PS1 mice (Fig. **2**), or this could be a consequence of the overexpression of mutant PS1 protein.

CONCLUSION

In conclusion, we identified several biological abnormalities that occur in the early stages of AD in the mouse hippocampus, including astrocyte activation, microglial activation, and extracellular matrix protein overexpression. We also detected the involvement of mTOR signaling and β-spectrin- and Rab3-mediated APP trafficking and proteolysis in early AD pathogenesis. Our results provide new insights into the early changes that occur in AD, and further identify candidate proteins as future early AD biomarkers or therapeutic targets.

LIST OF ABBREVIATIONS

AD	=	Alzheimer Disease
Aβ	=	β-Amyloid Peptide
APP	=	β-Amyloid Precursor Protein
2-DE	=	Two-Dimensional Gel Electrophoresis
iTRAQ	=	Isobaric Tags for Relative and Absolute Quantitation
GO	=	Gene Ontology
MF	=	Molecular Function
BP	=	Biological Process
CC	=	Cellular Component
Mag	=	Myelin-Associated Glycoprotein
Scn2b	=	Sodium Channel Subunit β-2
GFAP	=	Glial Fibrillary Acidic Protein
Mbp	=	Myelin Basic Protein
Col1a2	=	Procollagen, Type I, α-2
Calb2	=	Calretinin
Cdh13	=	Cadherin 13
Aip	=	AH Receptor-Interacting Protein
Dcakd	=	Dephospho-CoA Kinase Domain-Containing Protein
Atp2a1	=	Sarcoplasmic/Endoplasmic Reticulum Calcium ATPase 1

Efnb3 = Ephrin B3

Abca9 = ATP-Binding Cassette Subfamily A Member 9

Wdr77 = Methylosome Protein 50

GLT-1 = Glutamate Transporter-1

SIRT1/2 = Sirtuin 1/2

Prdx6 = Peroxiredoxin 6

Gstm1 = Glutathione S-Transferase μ-1

Uchl1 = Ubiquitin Carboxyl-Terminal Esterase L1

EFhd2 = EF-Hand Domain-Containing Protein D2

Nsf = N-Ethylmaleimide-Sensitive Factor

Dmxl2 = Rabconnectin-3

Rph3a = Rabphilin 3A

Sptbn1 = β-Spectrin

FUNDING

This work was supported by the National Key Basic Research Program of China (2013CB530904, 2015CB910801), National Natural Science Foundation of China (31571049, 81561168022) and the Fundamental Research Funds for the Central Universities of China.

AUTHOR CONTRIBUTION

N. Li performed the data analysis and the quantitative RT-PCR and shRNA knockdown experiments. Pinghong Hu performed some of the immune-blot experiments and data analysis. T. Xu, H. Chen, X. Xu, and J. Hu performed the iTRAQ experiments. X. Yang provided the 3xTg mice and performed the genotyping. Shi Lei and J-H Luo provided detailed discussions and suggestions for the project. J. Xu conceived the study and designed and coordinated the experiments. N. Li and J. Xu wrote the manuscript. All authors read and approved the final manuscript for submission.

ETHICS APPROVAL AND CONSENT TO PARTICIPATE

Not applicable.

HUMAN AND ANIMAL RIGHTS

No Animals/Humans were used for studies that are base of this research.

CONSENT FOR PUBLICATION

Not applicable.

CONFLICT OF INTEREST

The authors declare no conflict of interest, financial or otherwise.

ACKNOWLEDGMENTS

We sincerely thank Prof. Binggui Sun (Zhejiang University) and Prof. Fude Huang (Shanghai Advanced Research Institute, CAS) for generously providing the J20 and APP/PS1 mice. We also thank Prof. Huaxi Xu (Xiamen University) and Prof. Jianzhi Wang (Huazhong University of Science and Technology) for generously providing the N2A/APP695 cell line.

SUPPLEMENTARY MATERIAL

Supplementary Fig. **1**. Effect of Rab3a knockdown on APP surface expression and cleavage.

Supplementary Table **1**. Primers used for quantitative RT-PCR analysis of the expression of specific genes.

Supplementary Table **2**. List of proteins with a significant expression-level change of more than 20%.

Supplementary material is available on the publisher's web site along with the published article.

REFERENCES

[1] Sonkusare SK, Kaul CL, Ramarao P. Dementia of Alzheimer's disease and other neurodegenerative disorders-memantine, a new hope. Pharmacol Res 51(1): 1-17 (2005).

[2] Braak H, Braak E, Bohl J, Bratzke H. Evolution of Alzheimer's disease related cortical lesions. J Neural Transm Suppl 54: 97-106 (1998).

[3] Jack CR Jr., Petersen RC, O'Brien PC, Tangalos EG. MR-based hippocampal volumetry in the diagnosis of Alzheimer's disease. Neurology 42(1): 183-8 (1992).

[4] Poulin SP, Dautoff R, Morris JC, Barrett LF, Dickerson BC, Alzheimer's Disease Neuroimaging I. Amygdala atrophy is prominent in early Alzheimer's disease and relates to symptom severity. Psychiatry Res 194(1): 7-13 (2011).

[5] Jack CR, Jr., Petersen RC, Xu YC, Waring SC, O'Brien PC, Tangalos EG, *et al.* Medial temporal atrophy on MRI in normal aging and very mild Alzheimer's disease. Neurology 49(3): 786-94 (1997).

[6] Braak H, Braak E. Evolution of the neuropathology of Alzheimer's disease. Acta neurologica Scandinavica Supplementum 165: 3-12 (1996).

[7] Fox NC, Warrington EK, Freeborough PA, Hartikainen P, Kennedy AM, Stevens JM, *et al.* Presymptomatic hippocampal atrophy in Alzheimer's disease. A longitudinal MRI study. Brain 119 (Pt 6): 2001-7 (1996).

[8] Andreasen N, Vanmechelen E, Van de Voorde A, Davidsson P, Hesse C, Tarvonen S, *et al.* Cerebrospinal fluid tau protein as a biochemical marker for Alzheimer's disease: a community based follow up study. J Neurol Neurosurg Psychiatry 64(3): 298-305 (1998).

[9] Chartier-Harlin MC, Crawford F, Houlden H, Warren A, Hughes D, Fidani L, *et al*. Early-onset Alzheimer's disease caused by mutations at codon 717 of the beta-amyloid precursor protein gene. Nature 353(6347): 844-6 (1991).

[10] Selkoe DJ. Alzheimer's disease: genes, proteins, and therapy. Physiol Rev 81(2): 741-66 (2001).

[11] Ikeuchi T, Dolios G, Kim SH, Wang R, Sisodia SS. Familial Alzheimer disease-linked presenilin 1 variants enhance production of both Abeta 1-40 and Abeta 1-42 peptides that are only partially sensitive to a potent aspartyl protease transition state inhibitor of "gamma-secretase". J Biol Chem 278(9): 7010-8 (2003).

[12] Jacobsen H, Reinhardt D, Brockhaus M, Bur D, Kocyba C, Kurt H, *et al.* The influence of endoproteolytic processing of familial Alzheimer's disease presenilin 2 on abeta42 amyloid peptide formation. J Biol Chem 274(49): 35233-9 (1999).

[13] Ashford JW. APOE genotype effects on Alzheimer's disease onset and epidemiology. J Mol Neurosci 23(3): 157-65 (2004).

[14] Shaw LM, Vanderstichele H, Knapik-Czajka M, Clark CM, Aisen PS, Petersen RC, *et al.* Cerebrospinal fluid biomarker signature in Alzheimer's disease neuroimaging initiative subjects. Ann Neurol 65(4): 403-13 (2009).

[15] Hansson O, Zetterberg H, Buchhave P, Londos E, Blennow K, Minthon L. Association between CSF biomarkers and incipient Alzheimer's disease in patients with mild cognitive impairment: a follow-up study. Lancet Neurol 5(3): 228-34 (2006).

[16] Diamandis EP, Yousef GM, Petraki C, Soosaipillai AR. Human kallikrein 6 as a biomarker of alzheimer's disease. Clin Biochem 33(8): 663-7 (2000).
[17] Schonberger SJ, Edgar PF, Kydd R, Faull RL, Cooper GJ. Proteomic analysis of the brain in Alzheimer's disease: molecular phenotype of a complex disease process. Proteomics 1(12): 1519-28 (2001).
[18] Ross PL, Huang YN, Marchese JN, Williamson B, Parker K, Hattan S, *et al*. Multiplexed protein quantitation in Saccharomyces cerevisiae using amine-reactive isobaric tagging reagents. Mol Cell Proteom 3(12): 1154-69 (2004).
[19] Kolla V, Jeno P, Moes S, Tercanli S, Lapaire O, Choolani M, *et al*. Quantitative proteomics analysis of maternal plasma in Down syndrome pregnancies using isobaric tagging reagent (iTRAQ). J Biomed Biotechnol 2010: 952047 (2010).
[20] Zhou L, Beuerman RW, Chan CM, Zhao SZ, Li XR, Yang H, *et al.* Identification of tear fluid biomarkers in dry eye syndrome using iTRAQ quantitative proteomics. J Proteome Res 8(11): 4889-905 (2009).
[21] Manavalan A, Mishra M, Feng L, Sze SK, Akatsu H, Heese K. Brain site-specific proteome changes in aging-related dementia. Exp Mol Med 45(9): e39 (2013).
[22] Song F, Poljak A, Kochan NA, Raftery M, Brodaty H, Smythe GA, *et al*. Plasma protein profiling of Mild Cognitive Impairment and Alzheimer's disease using iTRAQ quantitative proteomics. Proteome Sci 12(1): 5 (2014).
[23] Martin B, Brenneman R, Becker KG, Gucek M, Cole RN, Maudsley S. iTRAQ analysis of complex proteome alterations in 3xTgAD Alzheimer's mice: understanding the interface between physiology and disease. PloS one 3(7): e2750 (2008).
[24] Mucke L, Masliah E, Yu GQ, Mallory M, Rockenstein EM, Tatsuno G, *et al*. High-level neuronal expression of abeta 1-42 in wild-type human amyloid protein precursor transgenic mice: synaptotoxicity without plaque formation. J Neurosci 20(11): 4050-8 (2000).
[25] Fu Y, Rusznak Z, Kwok JB, Kim WS, Paxinos G. Age-dependent alterations of the hippocampal cell composition and proliferative potential in the hAbetaPPSwInd-J20 mouse. J Alzheimer's Dis 41(4): 1177-92 (2014).
[26] Karl T, Bhatia S, Cheng D, Kim WS, Garner B. Cognitive phenotyping of amyloid precursor protein transgenic J20 mice. Behav Brain Res 228(2): 392-7 (2012).
[27] Meyer-Luehmann M, Spires-Jones TL, Prada C, Garcia-Alloza M, de Calignon A, Rozkalne A, *et al*. Rapid appearance and local toxicity of amyloid-beta plaques in a mouse model of Alzheimer's disease. Nature 451(7179): 720-4 (2008).
[28] Ashburner M, Ball CA, Blake JA, Botstein D, Butler H, Cherry JM, *et al*. Gene ontology: tool for the unification of biology. Gene Ontol Consortium. Nat Genet 25(1): 25-9 (2000).
[29] Consortium TGO. Gene Ontology Consortium: going forward. Nucl Acids Res 43(Database issue): D1049-56 (2015).
[30] Cho RJ, Campbell MJ. Transcription, genomes, function. Trends Genet 16(9): 409-15 (2000).
[31] Katoh K, Standley DM. MAFFT multiple sequence alignment software version 7: improvements in performance and usability. Mol Biol Evol 30(4): 772-80 (2013).
[32] Waterhouse AM, Procter JB, Martin DM, Clamp M, Barton GJ. Jalview Version 2--a multiple sequence alignment editor and analysis workbench. Bioinformatics 25(9): 1189-91 (2009).
[33] Moodley KK, Chan D. The hippocampus in neurodegenerative disease. Front Neurol Neurosci 34: 95-108 (2014).
[34] Desai MK, Sudol KL, Janelsins MC, Mastrangelo MA, Frazer ME, Bowers WJ. Triple-transgenic Alzheimer's disease mice exhibit region-specific abnormalities in brain myelination patterns prior to appearance of amyloid and tau pathology. Glia 57(1): 54-65 (2009).
[35] Power JH, Asad S, Chataway TK, Chegini F, Manavis J, Temlett JA, *et al.* Peroxiredoxin 6 in human brain: molecular forms, cellular distribution and association with Alzheimer's disease pathology. Acta Neuropathol 115(6): 611-22 (2008).
[36] Donmez G, Outeiro TF. SIRT1 and SIRT2: emerging targets in neurodegeneration. EMBO Mol Med 5(3): 344-52 (2013).
[37] de Mendonca E, Salazar Alcala E, Fernandez-Mestre M. Role of genes GSTM1, GSTT1, and MnSOD in the development of late-onset Alzheimer disease and their relationship with APOE*4. Neurologia 31(8): 535-42 (2016).
[38] Piacentini S, Polimanti R, Squitti R, Ventriglia M, Cassetta E, Vernieri F, *et al.* GSTM1 null genotype as risk factor for late-onset Alzheimer's disease in Italian patients. J Neurol Sci 317(1-2): 137-40 (2012).
[39] Pinhel MA, Nakazone MA, Cacao JC, Piteri RC, Dantas RT, Godoy MF, *et al*. Glutathione S-transferase variants increase susceptibility for late-onset Alzheimer's disease: association study and relationship with apolipoprotein E epsilon4 allele. Clin Chem Lab Med 46(4): 439-45 (2008).
[40] Chadwick W, Brenneman R, Martin B, Maudsley S. Complex and multidimensional lipid raft alterations in a murine model of Alzheimer's disease. Int J Alzheimers Dis 2010: 604792 (2010).
[41] Farina F, Botto L, Chinello C, Cunati D, Magni F, Masserini M, *et al.* Characterization of prion protein-enriched domains, isolated from rat cerebellar granule cells in culture. J Neurochem 110(3): 1038-48 (2009).
[42] Rockenstein E, Hansen LA, Mallory M, Trojanowski JQ, Galasko D, Masliah E. Altered expression of the synuclein family mRNA in Lewy body and Alzheimer's disease. Brain Res 914(1-2): 48-56 (2001).
[43] Beyer K, Domingo-Sabat M, Santos C, Tolosa E, Ferrer I, Ariza A. The decrease of beta-synuclein in cortical brain areas defines a molecular subgroup of dementia with Lewy bodies. Brain 133(Pt 12): 3724-33 (2010).
[44] Cirillo C, Capoccia E, Iuvone T, Cuomo R, Sarnelli G, Steardo L, *et al*. S100B Inhibitor Pentamidine Attenuates Reactive Gliosis and Reduces Neuronal Loss in a Mouse Model of Alzheimer's Disease. Biomed Res Int 2015: 508342 (2015).
[45] Mori T, Asano T, Town T. Targeting S100B in Cerebral Ischemia and in Alzheimer's Disease. Cardiovasc Psychiatry Neurol 2010 (2010).
[46] Griffin WS, Stanley LC, Ling C, White L, MacLeod V, Perrot LJ, *et al*. Brain interleukin 1 and S-100 immunoreactivity are elevated in Down syndrome and Alzheimer disease. Proc Natl Acad Sci USA 86(19): 7611-5 (1989).
[47] Choi J, Levey AI, Weintraub ST, Rees HD, Gearing M, Chin LS, *et al*. Oxidative modifications and down-regulation of ubiquitin carboxyl-terminal hydrolase L1 associated with idiopathic Parkinson's and Alzheimer's diseases. J Biol Chem 279(13): 13256-64 (2004).
[48] Ferrer-Acosta Y, Rodriguez-Cruz EN, Orange F, De Jesus-Cortes H, Madera B, Vaquer-Alicea J, *et al*. EFhd2 is a novel amyloid protein associated with pathological tau in Alzheimer's disease. J Neurochem 125(6): 921-31 (2013).
[49] Szodorai A, Kuan YH, Hunzelmann S, Engel U, Sakane A, Sasaki T, et al. APP anterograde transport requires Rab3A GTPase activity for assembly of the transport vesicle. J Neurosci 29(46): 14534-44 (2009).
[50] Rosengren LE, Wikkelso C, Hagberg L. A sensitive ELISA for glial fibrillary acidic protein: application in CSF of adults. J Neurosci Methods 51(2): 197-204 (1994).
[51] Fukuyama R, Izumoto T, Fushiki S. The cerebrospinal fluid level of glial fibrillary acidic protein is increased in cerebrospinal fluid from Alzheimer's disease patients and correlates with severity of dementia. Eur Neurol 46(1): 35-8 (2001).
[52] Crols R, Saerens J, Noppe M, Lowenthal A. Increased GFAp levels in CSF as a marker of organicity in patients with Alzheimer's disease and other types of irreversible chronic organic brain syndrome. J Neurol 233(3): 157-60 (1986).
[53] Colangelo AM, Alberghina L, Papa M. Astrogliosis as a therapeutic target for neurodegenerative diseases. Neurosci Lett 565: 59-64 (2014).
[54] Sihag RK, Cataldo AM. Brain beta-spectrin is a component of senile plaques in Alzheimer's disease. Brain Res 743(1-2): 249-57 (1996).
[55] Masliah E, Iimoto DS, Saitoh T, Hansen LA, Terry RD. Increased immunoreactivity of brain spectrin in Alzheimer disease: a marker for synapse loss? Brain Res 531(1-2): 36-44 (1990).
[56] Cai Y, Zhu HX, Li JM, Luo XG, Patrylo PR, Rose GM, et al. Age-related intraneuronal elevation of alphaII-spectrin breakdown product SBDP120 in rodent forebrain accelerates in 3xTg-AD mice. PloS one 7(6): e37599 (2012).
[57] Ayala-Grosso C, Tam J, Roy S, Xanthoudakis S, Da Costa D, Nicholson DW, *et al*. Caspase-3 cleaved spectrin colocalizes with neurofilament-immunoreactive neurons in Alzheimer's disease. Neuroscience 141(2): 863-74 (2006).

[58] Peterson C, Vanderklish P, Seubert P, Cotman C, Lynch G. Increased spectrin proteolysis in fibroblasts from aged and Alzheimer donors. Neurosci Lett 121(1-2): 239-43 (1991).

[59] Zhu HX, Xue ZQ, Qiu WY, Zeng ZJ, Dai JP, Ma C, *et al*. Age-related intraneuronal accumulation of alphaII-spectrin breakdown product SBDP120 in the human cerebrum is enhanced in Alzheimer's disease. Exp Gerontol 69: 43-52 (2015).

[60] Yan XX, Jeromin A. Spectrin breakdown products (SBDPs) as potential biomarkers for neurodegenerative diseases. Curr Transl Geriatr Exp Gerontol Rep 1(2): 85-93 (2012).

[61] Kobeissy FH, Liu MC, Yang Z, Zhang Z, Zheng W, Glushakova O, *et al.* Degradation of betaII-spectrin protein by calpain-2 and caspase-3 under neurotoxic and traumatic brain injury conditions. Mol Neurobiol 52(1): 696-709 (2015).

[62] Sakaguchi G, Orita S, Naito A, Maeda M, Igarashi H, Sasaki T, *et al*. A novel brain-specific isoform of beta spectrin: isolation and its interaction with Munc13. Biochem Biophys Res Commun 248(3): 846-51 (1998).

[63] Featherstone DE, Davis WS, Dubreuil RR, Broadie K. Drosophila alpha- and beta-spectrin mutations disrupt presynaptic neurotransmitter release. J Neurosci 21(12): 4215-24 (2001).

[64] Wang YP, Wang ZF, Zhang YC, Tian Q, Wang JZ. Effect of amyloid peptides on serum withdrawal-induced cell differentiation and cell viability. Cell Res 14(6): 467-72 (2004).

[65] Geppert M, Bolshakov VY, Siegelbaum SA, Takei K, De Camilli P, Hammer RE, *et al.* The role of Rab3A in neurotransmitter release. Nature 369(6480): 493-7 (1994).

[66] Geppert M, Goda Y, Stevens CF, Sudhof TC. The small GTP-binding protein Rab3A regulates a late step in synaptic vesicle fusion. Nature 387(6635): 810-4 (1997).

[67] Xu K, Zhong G, Zhuang X. Actin, spectrin, and associated proteins form a periodic cytoskeletal structure in axons. Science 339(6118): 452-6 (2013).

[68] Baines AJ, Lu HC, Bennett PM. The Protein 4.1 family: hub proteins in animals for organizing membrane proteins. Biochim Biophys Acta 1838(2): 605-19 (2014).

[69] Seabrook TJ, Bloom JK, Iglesias M, Spooner ET, Walsh DM, Lemere CA. Species-specific immune response to immunization with human versus rodent A beta peptide. Neurobiol Aging 25(9): 1141-51 (2004).

[70] Lopez-Toledano MA, Shelanski ML. Increased neurogenesis in young transgenic mice overexpressing human APP(Sw, Ind). J Alzheimers Dis 12(3): 229-40 (2007).

[71] Pomilio C, Pavia P, Gorojod RM, Vinuesa A, Alaimo A, Galvan V, *et al*. Glial alterations from early to late stages in a model of Alzheimer's disease: evidence of autophagy involvement in Abeta internalization. Hippocampus 26(2): 194-210 (2016).

[72] Borchelt DR, Ratovitski T, van Lare J, Lee MK, Gonzales V, Jenkins NA, *et al*. Accelerated amyloid deposition in the brains of transgenic mice coexpressing mutant presenilin 1 and amyloid precursor proteins. Neuron 19(4): 939-45 (1997).

[73] Kraft AW, Hu X, Yoon H, Yan P, Xiao Q, Wang Y, *et al.* Attenuating astrocyte activation accelerates plaque pathogenesis in APP/PS1 mice. FASEB J 27(1): 187-98 (2013).

[74] Moolman DL, Vitolo OV, Vonsattel JP, Shelanski ML. Dendrite and dendritic spine alterations in Alzheimer models. J Neurocytol 33(3): 377-87 (2004).

[75] Webster SJ, Bachstetter AD, Nelson PT, Schmitt FA, Van Eldik LJ. Using mice to model Alzheimer's dementia: an overview of the clinical disease and the preclinical behavioral changes in 10 mouse models. Front Genet 5: 88 (2014).